

Geometrical effects in the intermediate state of type-I Pb superconductors

Author: Carla Barceló-Sàbat

Advisor: Antoni García-Santiago

*Facultat de Física, Universitat de Barcelona, Diagonal 645, 08028 Barcelona, Spain**

The influence of geometry on the nature of the intermediate state in superconducting type-I lead is presented. Isothermal measurements of first magnetization curves and hysteretical cycles of several cylindrical samples show an irreversible region when the magnetic field, parallel to the axis of revolution, decreases from the normal state. Comparing data for samples with different aspect ratio –length divided by diameter- has proved the existence of a geometrical barrier due to the shape and the orientation of the sample that strongly determines the behaviour of the magnetic flux. Finally, an analysis of the thermal dependence of the critical field, the irreversible field and the remnant magnetization for each sample is given in order to reinforce the idea that geometrical barriers are the fundamental cause of irreversibility.

I. INTRODUCTION

Since the beginning of the 19th century, the magnetic behaviour of type-I superconductors has been the subject of study of many scientists. Landau was pioneering in describing the structure of intermediate state that is produced when, over a critical magnetic field, the magnetic flux is able to penetrate this kind of materials creating a region of coexistence of normal and superconducting phases [1-2]. One of the highlights of the theory is the emergence of irreversibility for flux penetration and flux expulsion in this intermediate state.

Initially, the irreversibility of the process was associated with the presence of defects or impurities in the sample [3]; however, recent experiments have revealed that extremely pure samples without any defect also exhibit a similar performance [4-6]. This reality encouraged the search of new sources of irreversibility.

In this context, it is plausible to think that the topology of flux penetration –tubular regime- and flux expulsion –laminar regime- is closely correlated with irreversibility. This phenomenology is attributed to the presence of a geometrical barrier in structures that present two parallel plane surfaces perpendicular to the applied magnetic field. Their effects will be modified depending on the distance between the surfaces –cylinder length- and on their orientation. In the same way, they will vanish for zero field or for magnetic fields perpendicular to the axis of revolution [4-7].

Another factor that plays an important role in superconductor's hysteresis cycles is the temperature. Latest observations suggest that the trapping of normal-superconductor interfaces in defects –only present under the influence of a geometrical barrier- shows a thermal dependence manifested by a reduction of irreversible field and remnant magnetization as the temperature increases. In contrast, it seems that the geometrical barrier is not affected by this variable [8].

Nevertheless, everything seems to indicate that the geometrical barrier is the main cause of irreversibility in this kind of type-I superconductors. This is the reason why a set of cylindrical samples with different aspect ratio will be analysed in order to deeply study how the variation of geometry could modify the hysteresis cycle, the remnant magnetization in zero field and the irreversibility of the intermediate state.

Isothermal magnetization curves have been obtained for some lead samples with decreasing aspect ratio –from cylinders to disks- at several temperatures and they will be compared and scaled in terms of dimensionless reduced magnitudes to focus the study on geometrical effects. This representation should evidence behaviours previously described and accurately define the impact of the geometry of the sample in the intermediate state characterization, particularly in its irreversibility.

II. EXPERIMENTAL SETUP

Table I contains the lengths of the different cylindrical lead samples that have been analysed. They have been labelled progressively from 1 to 6 in a way that the first one has the appearance of a cylinder and the last one of a disk. All of them have been obtained from the same commercial rod of extremely pure lead (99,999 at. %) ¹ by cutting consecutively with a mechanical saw blade of 1 mm of thickness. The diameter of all samples is $3,56 \pm 0,02$ mm.

Sample	Length (mm)
1	6,00±0,02
2	3,96±0,02
3	2,96±0,02
4	1,86±0,03
5	0,93±0,01
6	0,62±0,02

TABLE I: Length data for cylindrical lead superconducting samples.

In order to avoid surface rust, all the samples received the same chemical treatment: they were submerged in a HCl 1N solution for 2 or 3 minutes, washed with water for 2 minutes and, afterwards, with acetone for another 2 minutes. Finally, they were stored in vacuum until further usage.

The magnetic measurements were performed in a magnetometer based on a superconducting quantum interference device known as SQUID². This type of equipment allows to apply magnetic fields up to 5 T of intensity and work in temperatures as low as 1.8 K.

¹ Alfa Aesar (lead rod, $3,56 \pm 0,02$ mm diameter)

² Magnetic Properties Measurement System, Quantum Design, San Diego.

* Electronic address: carlabs.95@gmail.com

To achieve these conditions, the magnetometer has a superconducting magnet that provides the desired intensity and a helium refrigerating circuit. Detection coils, together with the SQUID permit us to evaluate the magnetic signal of the sample and its translation, by using proper algorithms, into the corresponding magnetization value with a resolution up to 10^{-5} emu.

Regarding data collection, the samples were first cooled from normal state in zero magnetic field (Zero Field Cooling process) down to the desired temperature value, and in the same way, after the measurement in a specific temperature the sample was heated over the critical temperature in order to eliminate the remnant magnetization that could alter the next set of data.

Following this procedure for each cylinder and temperature –steps of 0.5 K in a range from 2 to 7 K– first magnetization curves $M_{1st}(H)$ and descending branches of the cycle $M_{des}(H)$ have been obtained. The record of the entire hysteresis cycle has been avoided because of its symmetry and with the aim of saving helium and time in the data collection. It is necessary to remark that all the measurements have been done under a magnetic field applied parallel to the axis of revolution of the samples.

III. RESULTS AND DISCUSSION

A. Hysteresis cycles

Figure 1 presents hysteresis cycles for the different samples at $T = 2$ K. In panel (a) magnetization curves $M(H)$ have been normalised to the maximum value of magnetic field attained along the cycle –that corresponds to the critical field H_c – in such a way that magnetization data become $m=M/H_c$ and $h=H/H_c$. In panel (b), in order to focus on geometrical effects, the analysis has been taken one step further and data have been also normalised to the maximum magnetization value, m_{max} , as $m^*=m/m_{max}$. In this way, h and m^* are dimensionless magnitudes³.

At first sight, all the cycles exhibit several common features. Initially, all of them show a linear regime, known as Meissner state, along $M_{1st}(H)$ up to a specific value, h' , at which magnetization reaches its minimum. For higher values, the flux begins to penetrate the superconductor and induces the intermediate state while the magnetization tends to decrease and becomes zero at the critical field. As the field decreases along the $M_{des}(H)$ branch, a reversible region appears up to a certain h^* value –commonly called reduced irreversible field– below which $M(H)$ separates from $M_{1st}(H)$. Therefore, the magnetization describes an alternative path until it reaches its maximum and decreases again to zero.

The representation evidences how all this values change depending on the geometry of the sample. In the first place, the Meissner state is larger in cylinders than in disks; in other words, the intermediate field h' is reduced as the length decreases: sample 1 shows $h' \sim 0,9$ whereas sample 6 presents $h' \sim 0,35$. This result is consistent with the fact that demagnetizing factor, N , increases correspondingly [9]. To check this, experimental and theoretical N values have been calculated for each sample using the data obtained and the

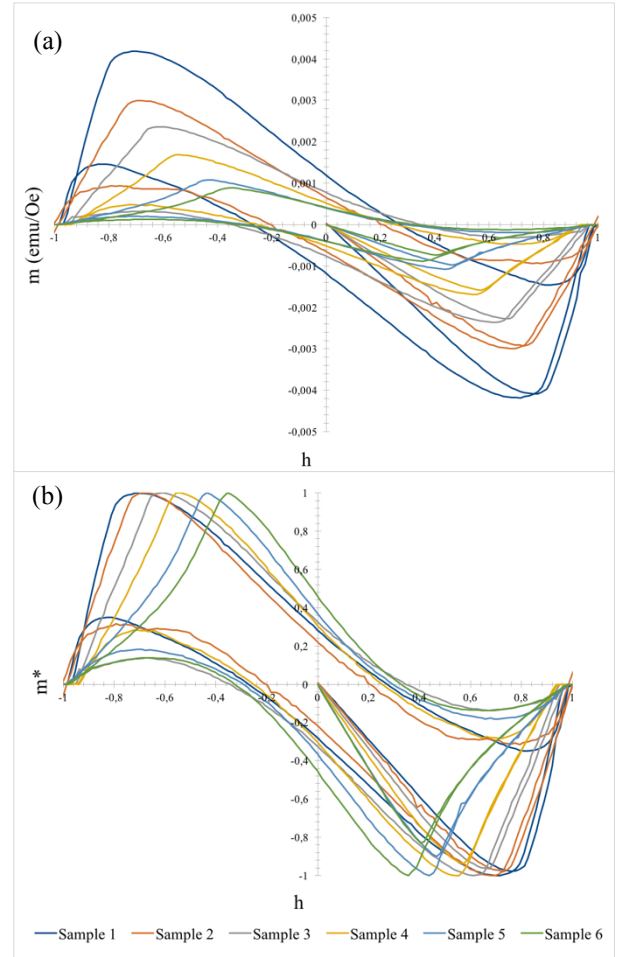


FIG. 1: First magnetization curves and magnetic hysteresis cycles measured on sample 1 to 6 at $T = 2.00$ K in terms of reduced magnitudes $m(h)$ -Panel (a)- and $m^*(h)$ -Panel (b).

following equations, where n is the so-called aspect ratio, that is the quotient between the length and the diameter:

$$H' = H_c \cdot (1 - N_{exp})$$

$$N_{theo} = \frac{1}{2\left(\frac{2n}{\sqrt{\pi}}\right)+1} \quad (1)$$

A comparison between theoretical and experimental values –Table II- manifests that N_{exp} is close to the expected one, $N \sim 1/3$ in cylinders and $N \sim 9/10$ in disks [10].

Sample	Aspect ratio n	N_{exp}	N_{theo}
1	$1,68 \pm 0,02$	$0,238 \pm 0,006$	$0,218 \pm 0,001$
2	$1,11 \pm 0,01$	$0,281 \pm 0,005$	$0,285 \pm 0,002$
3	$0,83 \pm 0,01$	$0,330 \pm 0,019$	$0,348 \pm 0,003$
4	$0,52 \pm 0,01$	$0,414 \pm 0,015$	$0,459 \pm 0,005$
5	$0,261 \pm 0,004$	$0,537 \pm 0,008$	$0,629 \pm 0,004$
6	$0,174 \pm 0,007$	$0,598 \pm 0,006$	$0,718 \pm 0,008$

TABLE II: Aspect ratio, n , experimental, N_{exp} , and theoretical, N_{theo} , demagnetizing factor for 1 to 6 cylindrical lead superconducting samples. N_{exp} is the average of the values obtained for all the temperatures in each sample.

³ Hysteresis cycle for $T = 2$ K has been chosen to illustrate the general behaviour in all the samples since all the cycles obtained at different temperatures are very similar.

In the second place, remnant magnetization can be appreciated in all the samples, in particular for the shortest lengths. This may be attributed to the presence of structural defects in this type of samples, so in a lack of them, remnant magnetization is practically zero for cylinders [7].

Finally, it is interesting to notice that the maximum magnetization decreases around 80 % as the length shortens [Fig. 1(a)].

B. $H_c(T)$ dependence

Figure 2 shows the thermal dependence of the critical field, H_c . As expected, it reduces as the temperature increases; that means the sample would become normal in a lower field value. On the basis of the graph we may calculate the critical temperature and the critical field value at $T = 0$ K for each sample using the following equation [11]:

$$H_c(T) = H_c(0) \left[1 - \left(\frac{T}{T_c} \right)^2 \right] \quad (2)$$

The averages obtained over all the samples are $T_c = 7.24 \pm 0.07$ K and $H_c(0) = 829 \pm 13$ Oe. These values are consistent with reference figures found in the literature, $T_c = 7.19$ K and $H_c(0) = 800$ Oe [12].

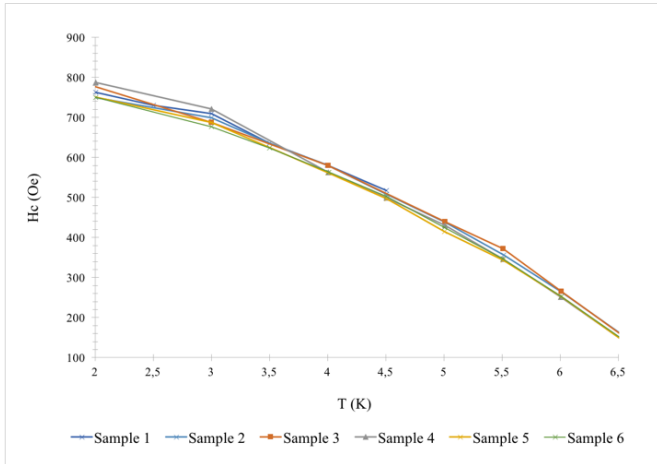


FIG. 2: Temperature dependence of the critical field, $H_c(T)$ for each sample studied.

C. Irreversibility: $m_{\text{rem}}(T)$ and $h^*(T)$

If one looks at the evolution of the hysteresis cycles for each sample at several temperatures –figure 3-, it seems that they widely overlap, especially along the first magnetization curve, suggesting that flux penetration is thermal independent for both cylindrical and disk-shaped samples⁴.

Nevertheless, the irreversible region does not exhibit such behaviour, and so the magnetization curve follows different path depending on the temperature. In disk samples, the path variation is larger than in the case of cylinders. As it has been said before, even though all samples are made of extremely pure lead, the irreversibility could be attributed to the occurrence of defects; otherwise, if it was caused exclusively by geometrical barriers, the cycles should overlap [7].

⁴ Figure 3 only includes the hysteresis cycle of sample 1 –the largest one- and sample 6 –the shortest one- at several temperatures because Treball de Fi de Grau

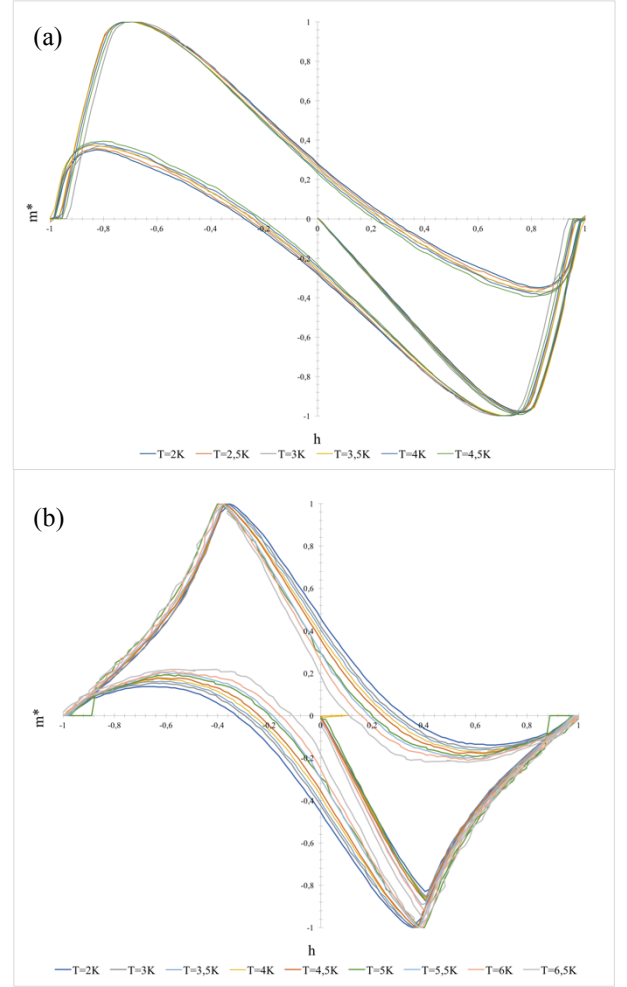


FIG. 3: First magnetization curves and magnetic hysteresis cycles measured on sample 1 –panel (a) – and sample 6 –panel (b) – at several temperatures in a range from $T = 2.00$ K to $T = 6.50$ K. Data are plotted in terms of reduced magnitudes $m^*(h)$.

Since defects come into play, normal-superconducting interfaces (NSI) can be pinned and therefore they have to overcome pinning energy barriers to move through the sample. As the magnetic field decreases in flux expulsion, the interfaces would lose energy as a result of dissipative processes until they would be pinned by the defects. In contrast, thermal independence during flux penetration seems to indicate that pinning and depinning of NSI are not relevant at the macroscopic scale, leaving aside their role in the formation of flux patterns [8].

Consequently, pinning effects and the fact that they are more important in disks than in cylinders help to understand the occurrence of different hysteresis cycle areas and their variation with the temperature. Moreover, the onset of irreversibility at h^* when h decreases induces thermal activation processes which are necessary to release the NSI from the pinning. According to the Arrhenius equation, the frequency of this kind of process presents an exponential decline with the effective pinning energy barrier, $U(h)$. It is important to remark that, in the time scale of our measurements, this kind of processes becomes relevant when $U(h) \sim 25k_B T$ [8]. With regard to all these considerations, it is conceivable to think that $h^*(T)$ and $U(h)$ present the same

they are the most representative to illustrate the behaviour of a cylindrical and disk-shaped sample.

dependence; in other words, the higher the energy barrier at certain temperature, the larger the irreversible field will be.

Panel (a) in figure 4 presents the thermal dependence of the irreversible field, $h^*(T)$. In this particular case, there is not an evident variation among samples and this could mean that they have similar energy barriers. Panel (b) in the same figure illustrates a decreasing thermal dependence of the remnant magnetization, which seems to be more relevant in disks. However, the remnant magnetization at a certain temperature barely varies with the length of the sample [Fig. 1 (b)]. The only thing that seems to be clear is that the shortest cylinder, sample 6, presents the largest remnant magnetization, which could be due to a combination of a higher geometrical barrier and an excess of manufacturing defects. Maybe these stress defects were induced during the preparation process of such a thinner sample.

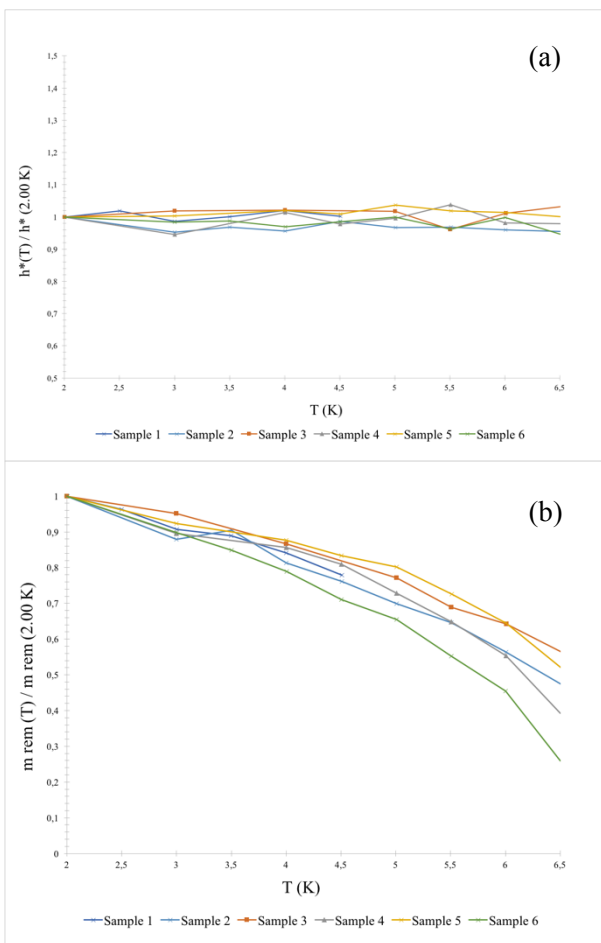


FIG. 4: Temperature dependence of the reduced irreversible field, $h^*(T)$, –panel (a)- and temperature dependence of the reduced remnant magnetization, $m^*(T)$, –panel (b)- for each sample studied. Both representations are normalized to their values at 2.00 K.

As the remnant magnetization is correlated to defects, and these to the pinning energy barriers which fix the onset of the irreversible field, it can be assumed that the relative variation of remnant magnetization, $m_{\text{rem}}(T)$ is mostly determined by the

relative variation of irreversible field, $h^*(T)$. However, the results obtained present a great variation of $m_{\text{rem}}(T)$ –which is reduced 40 % at least and 70 % at most- but not for $h^*(T)$. It seems that this reduction is quite similar among all the samples –maybe with the exception of sample 6–, so it is plausible to think that all of them have similar energy barriers correlated with different defects distribution, which do not produce important changes from one sample to another.

IV. CONCLUSIONS

In conclusion, the geometry of the sample strongly determines the intermediate state’s phenomenology of type-I superconductors. In particular, the modification of the length of the cylinder has manifested changes both in isothermal magnetization curves and their evolution for different temperatures.

Firstly, it has been proven that the onset of the intermediate state appears at lower fields as the aspect ratio of the cylinder decreases –or either the demagnetizing factor increases. Secondly, the remnant magnetization enlarges for disks, which seems to mean that flux pinning by defects is more remarkable in this kind of shape. In the same way, it also has been possible to observe how the temperature plays a different role depending on the geometry.

Moreover, the analysis of such role in different shapes has allowed to define, a little further, its influence on the critical field, the remnant magnetization and the irreversible field. On the one hand, we have been able to verify the expected behaviour of $H_c(T)$ by the theoretical model, seeing that experimental values of critical temperature and remnant magnetization at zero field are close to those found in the literature.

On the other hand, contrary to expectations, while the remnant magnetization varies considerably depending on the temperature, the onset of the irreversible field does not exhibit any substantial modification. In any case, as the variation of the remnant magnetization is quite similar for all the samples, it can be argued that all of them present similar energy barriers so they must have also similar irreversible fields.

The next step that could be done in order to investigate the cause of the $h^*(T)$ and the $m_{\text{rem}}(T)$ behaviour, would be to measure the magnetic relaxations in all the samples to observe if the remnant magnetization varies considerably along the time. If so, the existence of pinning barriers associated with defects would be confirmed, supporting the previous predictions.

Acknowledgments

I would like to express my gratitude to my advisor Antoni García-Santiago for his continued guidance, his clear explanations and his inestimable help during the elaboration of this study. I also want to thank my family and friends for their support and their confidence in me during all this time.

- [1] Landau L D, «Theory of supraconductivity,» 1937 *Zh. Eksp. Teor. Fiz.* **7** 371
- [2] Landau L «The intermediate state of supraconductors,» 1938 *Nature* **141** 688
- [3] Livingston J D and DeSorbo W 1969 *Superconductivity* vol 2, ed R D Parks (New York: Dekker) p. 1235 and references therein
- [4] Prozorov R, Giannetta R W, Polyanskii A A and Perkins G K, «Topological hysteresis in the intermediate state of type-I superconductors,» 2005 *Phys. Rev. B* **72** 212508
- [5] Prozorov R, «Equilibrium topology of the intermediate state in type-I superconductors of different shapes,» 2007 *Phys. Rev. Lett* **98** 257001
- [6] Hoberg J R and Prozorov R, «Current-driven transformations of the intermediate-state patterns in type-I superconductors,» 2008 *Phys. Rev. B* **78** 104511
- [7] Vélez S, Panadès-Guinart C, Abril G, García-Santiago A, Hernandez J M and Tejada J, «Topological magnetic irreversibility in superconducting Pb samples of various shapes,» 2008 *Phys. Rev. B* **78** 134501
- [8] Vélez S, García-Santiago A, Hernandez J M and Tejada J, «The role of temperature in the magnetic irreversibility of type-I Pb superconductors,» 2012 *J. Phys: Condens. Matter* **24** 485701
- [9] Rose-Innes A C and Rhoderick E H 1978 *Introduction to Superconductivity* (Oxford: Pergamon) p. 70
- [10] Sato M and Ishii Y, «Simple and approximate expressions of demagnetizing factors of uniformly magnetized rectangular rod and cylinder,» 1989 *J. Appl. Phys.* **66** 983
- [11] Tinkham M 2004 *Introduction to Superconductivity* (New York: Dover) p. 3
- [12] Flükiger R, Hulliger F, Kaner N, Luo H L, Müller R, Radhakrishnan T S, Shelton R N, Weis F, Wolf T and Yu D 1997 *Superconductors: Transition Temperatures and Characterization of Elements, Alloys and Compounds: O (without cuprates)-Sc* (Landolt-Börnstein New Series vol III/21c) ed R Flükiger and W Klose (Heidelberg: Springer-Verlag) p. 29